

NJC

Accepted Manuscript



This is an *Accepted Manuscript*, which has been through the Royal Society of Chemistry peer review process and has been accepted for publication.

Accepted Manuscripts are published online shortly after acceptance, before technical editing, formatting and proof reading. Using this free service, authors can make their results available to the community, in citable form, before we publish the edited article. We will replace this *Accepted Manuscript* with the edited and formatted *Advance Article* as soon as it is available.

You can find more information about *Accepted Manuscripts* in the [Information for Authors](#).

Please note that technical editing may introduce minor changes to the text and/or graphics, which may alter content. The journal's standard [Terms & Conditions](#) and the [Ethical guidelines](#) still apply. In no event shall the Royal Society of Chemistry be held responsible for any errors or omissions in this *Accepted Manuscript* or any consequences arising from the use of any information it contains.



www.rsc.org/njc

Electrochemical synthesis of TiC reinforced Fe based composite powder from Titanium-rich slag

Sun Lin¹, Song Qiushi¹, Xu Qian^{2*}, NingZhiqiang¹, Lu Xionggang², Fray Derek³

¹School of Materials Science and Metallurgy, Northeastern University, Shenyang 110004, China

²School of Materials Science and Engineering, Shanghai University, Shanghai 200072, China

³Department of Materials Science and Metallurgy, University of Cambridge, Cambridge, CB3 0FS, UK

Abstract

TiC reinforced Fe based composite powder was electrochemically prepared directly from the titanium-rich slag and carbon in molten $\text{CaCl}_2\text{-NaCl}$ at 800°C . The reaction pathway from the slag and carbon to TiC-Fe based composite powder was investigated by examination of partially and fully reduced samples using XRD and SEM with EDS analyses. The process of reduction and carbiding process can be divided into the two main stages. The first stage of the process is the electrochemical reduction, while the second stage is a synergetic reaction of the electrochemical de-oxidation and carbiding. During the second stage, the TiC forms from $\text{TiC}_x\text{O}_{1-x}$, in which the carbon atoms substitute for oxygen atoms successively to stoichiometric TiC. The TiC grains initiate the heterogeneous nucleation for the TiC-Fe based alloy particles with multi-core microstructure.

Keywords: TiC-Fe composite, electro-deoxidation, molten salt, carbiding, reaction pathway

1. Introduction

Fe-TiC composite has attracted a lot of attentions due to its unique properties, such as high strength and hardness, good chemical and thermal stability. In general, the main application of Fe-TiC composite is as a wear resistant material. It has been demonstrated that the wear resistance of the material increases with the decrease in the particle size of TiC, and the increase in the volume fraction of carbide in the composite^[1].

Conventionally, the powder metallurgy route has been used widely to produce Fe-TiC composite^[2-3]. It involves the addition of TiC powder to iron powder which offers the possibility to produce the composite with a very fine and high volume fraction of TiC. However, production of the composite via the powder metallurgy route has some limitations^[4]. Therefore, many other routes involving in-situ generation of the reinforcing phase were proposed such as the melting and casting route^[5,6], carbothermic reduction^[7] and combustion synthesis^[8-10]. However, it is difficult for these techniques to produce the finer ceramic particles because the high reaction temperature will lead to coarsening of the ceramic particles. Meanwhile, the mechanical alloying route seems to be one of the effective methods to prepare the fine TiC powder^[11-13]. However, the particles prepared by the mechanical alloying process should have a great number of defects within the crystalline solid, especially on their surface structure, which induces the individual particles easily to form larger aggregates.

There is still a big problem for TiC powder to serve as a reinforced phase due to its

low wettability to the metal matrix. A core-rim microstructure of the TiC particles was reported to improve the wetting and sinterability of the composite^[14-16]. However, studies on TiC particles sealed in the metal matrix particles with multi-core microstructure have been seldom reported.

A novel electrochemical process has been developed by the scientists of the University of Cambridge (so called FFC Cambridge process), and different metals and alloys was successfully prepared directly from their oxides^[17-19]. Recently, the preparation of nano-crystalline carbide powders have been also attempted by the FFC process^[20], using the oxide and carbon powders as the raw materials. In this case, the molten salt served as the electrolyte for the electrochemical de-oxidation. Furthermore, the temperature for preparing the carbide in the molten salt is significantly lower than that employed in the powder metallurgy route. The considerably low operating temperature and good dispersity of particles are important factors for successful synthesis of the nano-sized carbide particles.

In this work, we investigated electrochemical synthesis of TiC reinforced Fe-based composite with multi-core microstructure from titanium-rich slag in the molten CaCl₂-NaCl at 800 °C. The TiC-Fe based powder was characterized by X-ray diffraction (XRD) and scanning electron microscopic (SEM) analyses. The possible reaction pathway of the electrochemical reaction was obtained by examination of the partially reduced samples after various durations using XRD analysis.

2. Experimental

A titanium-rich slag was prepared by reaction between ilmenite and coal in electric furnace, and it was provided from the Titanium Plant of Panzhihua Iron and Steel Group Corporation, Sichuan in China. The titanium-rich slag blocks were crushed and examined by XRD analysis, as shown in Fig. 1a. The chemical composition was analyzed by X-ray Fluorescence Spectroscopy (RIGAKU, ZSX100e), and the result was listed in Table 1.

Table 1

The composition of titanium-rich slag as received

Components	TiO ₂	Fe ₂ O ₃	SiO ₂	Al ₂ O ₃	MgO	MnO	CaO
Concentration (wt%)	69.6	16.3	7.87	2.0	1.37	1.31	0.76

A mixture of titanium-rich slag and carbon black was milled in a conventional ball-mill pot using a stainless steel ball for 10min. The contents of carbon black in the raw material were set to 5% and 10% in mass. About 1.0g of the mixture of titanium-rich slag and carbon black was compacted into a cylindrical pellet of 15mm in diameter and 1.5mm in thickness under 10MPa. Then, the pellets were sintered at 800, 1000, or 1200°C for 4h in an argon atmosphere.

A eutectic mixture of CaCl₂-NaCl, which served as the electrolyte, was first thermally dehydrated at 300°C for 24h and then melted at 800°C in an alumina crucible, which was contained in the stainless reactor in argon atmosphere. In order to remove the electrochemical-active impurities from the melt, pre-electrolysis of the melt was carried out at 3.0V for 2h, during which two graphite rods were employed as an anode and a cathode. After the pre-electrolysis, the sintered slag-carbon pellet was immersed slowly into the melt as the cathode instead of the graphite cathode,

and the electrochemical reduction was performed at the potential of 3.1V. Partially and fully reduced samples were obtained by terminating the electrochemical reduction after different durations from 2 to 24h. More experimental details were similar to those described in the previous work^[21].

The products were characterized by X-ray diffractometry with Cu K α radiation, and their morphologies were examined by means of an SSX-550 scanning electron microscope equipped with energy-dispersive X-ray analysis.

3. Results and discussion

3.1 Cathode preparation

Fig. 1 shows the typical XRD patterns for the as-received rich-titanium slag and the titanium-rich slag-carbon mixtures sintered at 800, 1000, and 1200°C, respectively. The XRD patterns in Fig. 1(b) and (c) show an Anosovite of M₃O₅ (M=Ti, Fe) as the main crystalline phase in the mixtures when the sintering temperature is 1000°C or lower. It is the same as the as-received slag shown in Fig.1(a). Moreover, the weight loss of the sintered pellets was less than 1 wt% which means that there are few reactions between the slag and carbon during the sintering process when the temperature is not higher than 1000°C. Meanwhile, there are no peaks corresponding to carbon probably because the carbon black used in this study should have amorphous structure. For the sample sintered at 1200°C, the typical peak of Fe can be detected from the XRD pattern shown in Fig.1(d), suggesting that some ferrous oxide is reduced from M₃O₅(M=Ti, Fe) and form elemental Fe, while TiO₂ is reduced to Ti₃O₅ as described by equation (1) at 1200°C. These reductions lead to the

predominance phase of M_3O_5 still existing in the mixture, and no TiO_2 detected in the XRD pattern in Fig.1(d). However, the further reduction of Ti_3O_5 is less preferable thermodynamically at $1200^\circ C$ according to the equation (2).

In the preparation of the slag-carbon cathode for TiC reinforced Fe based composite in this work, the sintering temperature was then set to $1000^\circ C$ in order to use carbon black as the carbon source for the carbide formation rather than a reduction agent.

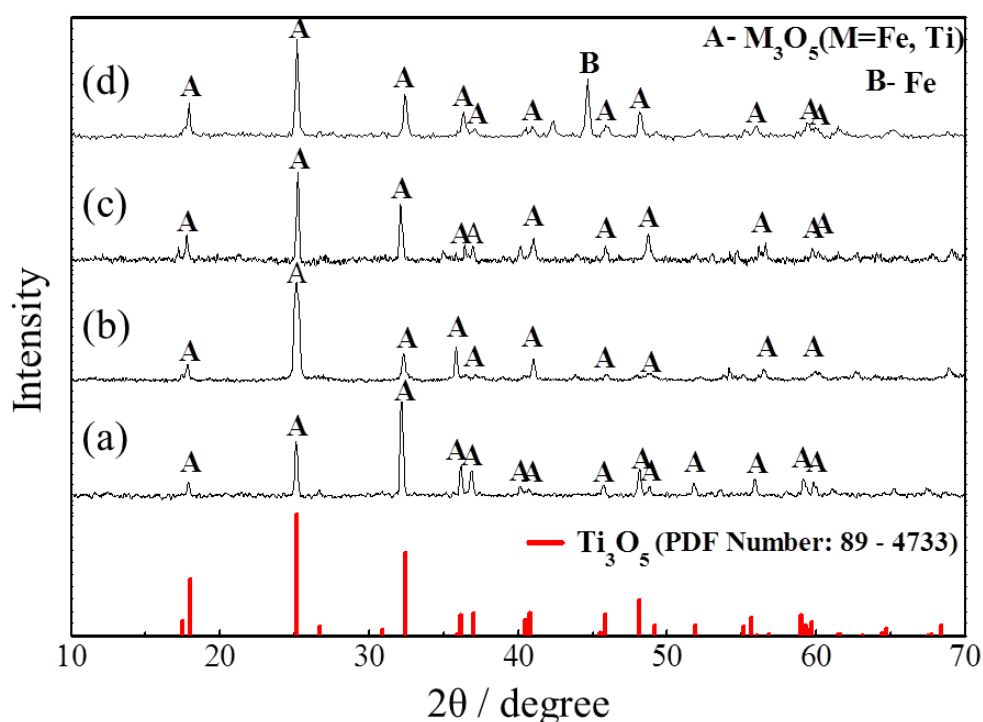
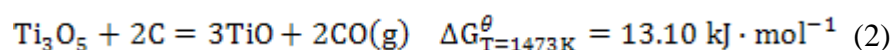
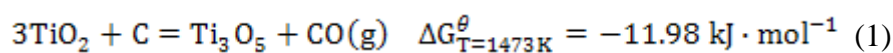


Fig.1. The XRD patterns of (a) the titanium-rich slag and the titanium-rich slag-C mixtures sintered at (b) $800^\circ C$, (c) $1000^\circ C$ and (d) $1200^\circ C$ for 4h.

Fig. 2(a) shows the morphology of the pellet made of the slag with 5 wt% carbon powder after the 4h-sintering process at $1000^\circ C$. It has a coarse microstructure, in

which most slag particles are dense and monolithic. Fig. 2(b) shows the SEM image in a bigger magnification for the labeled area in Fig. 2(a). The fine powder among the coarse slag particles should be the carbon powder.

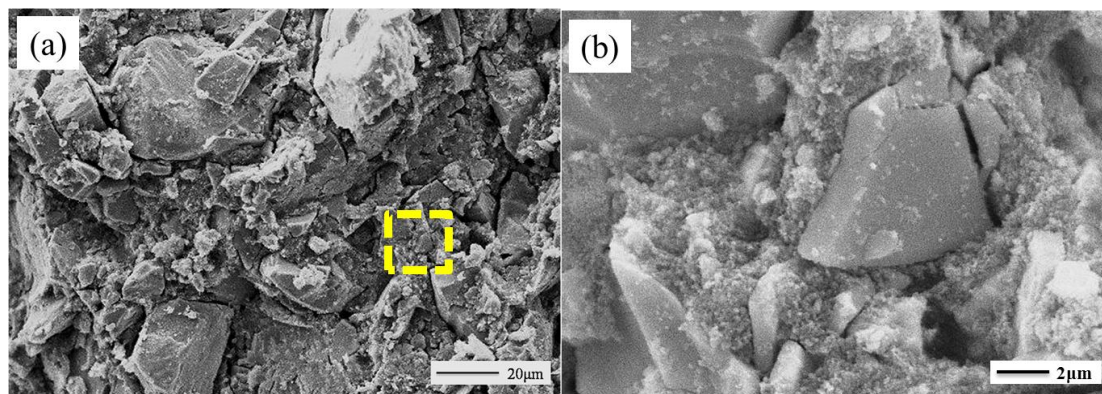


Fig.2 (a) SEM image of the pellet made of the slag with 5 wt % carbon sintered at 1000°C for 4h ; (b) The microstructure of the labeled area in fig. 2(a).

3.2 Phase identification of the reduced samples

After the 24h-electrolysis, the electrochemical reduction and carbonization of the titanium-rich slag at 800°C have been achieved. Fig. 3(a) shows the XRD pattern for the product from the sample containing 5wt% carbon. The product contains the two kinds of phases, one is the ceramic phase of TiC, and the other is metal phase of FeTi and Ti₅Si₃. When the carbon content in the sample increases up to 10wt%, SiC can be detected in addition to TiC from the XRD pattern shown in Fig. 3(b). Correspondingly, only Fe is involved in the metal phase. It indicates that Si can transfer from Ti₅Si₃ alloy to the carbide. As shown in table 1, the main elements in the titanium-rich slag are Ti, Fe, Si and O, in which oxygen atoms bind all the other atoms. During the cathodic polarization of the slag with the presence of carbon in the molten salt at 800°C, the electro-deoxidation of the oxides can be achieved. That means oxygen atoms in the cathode can be removed to the molten salt, whilst the

atoms of Ti, Fe, Si and C can remain in the cathode. The XRD patterns in Fig.3 indicate that transformation of Ti to TiC is most preferential, while other elements exist in the form of metal phases, when the amount of carbon is deficient within the slag. Furthermore, the formation of SiC is the secondly most preferential, and only Fe is left in the metal phase when the content of carbon is increased up to 10wt% as shown in Fig.3. The findings are in good agreement with the Gibbs energy changes calculated for the corresponding reactions shown in equation (3)-(5) at 800°C.

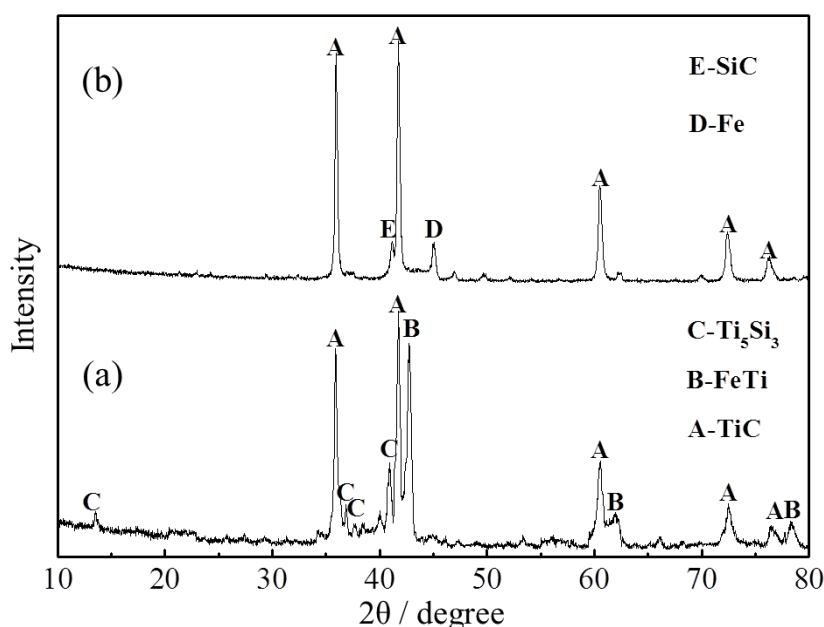
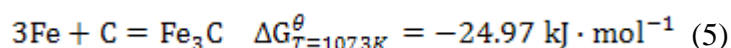
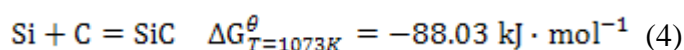
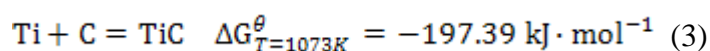
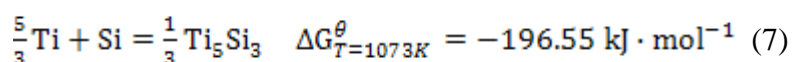


Fig.3 XRD patterns of the pellets with (a) 5wt% C and (b) 10% C electrolyzed for 24h.

It is concluded that the composition of the carbides in the final product can be

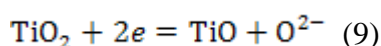
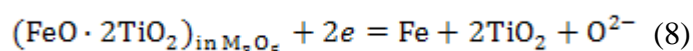
controlled by adjusting of the amount of carbon in the titanium-rich slag precursor. It is also found that Si is favorable to form Ti_5Si_3 in comparison with Fe. This can be explained by their formation free energy shown in equation (6) and (7).

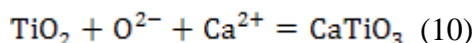


3.3 The reaction pathway

To investigate the mechanism for the formation of TiC-Fe based composite, a series of the partially reduced slag with the different contents of carbon (5wt% and 10wt%) were determined by XRD, and are shown in Fig. 4. The process of reduction and carbiding basically occurred in the two main stages.

In the stage I, during the first 2h of the process, the typical peaks of $(\text{Fe,Ti})_3\text{O}_5$ are eliminated, while the peaks for Fe, TiO_2 , CaTiO_3 , and TiO appear. However, there is no peak for any carbides, implying that the initial reaction in the cathode is the oxygen removal and combination with CaO rather than carbiding. The possible cathode reductions are as described as equation (8) - (10). Although the contents of carbon are 5wt% and 10wt% in the samples, their XRD patterns are quite similar to each other, indicating that there is few effect of carbon on the initially electrochemical reduction of the cathode besides introducing a conductive phase throughout the cathodic pellets.





During the first stage, almost all the ferric oxides in the cathode can be electrochemically reduced, which leads to a higher electric conductivity for the cathode than the initial material.

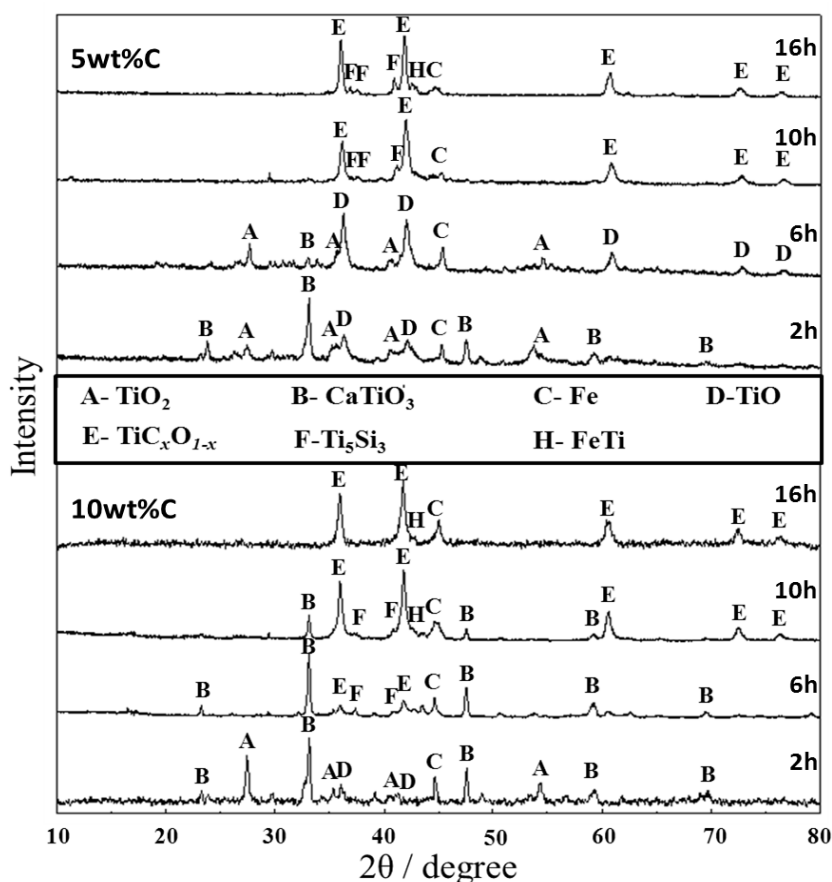


Fig.4. XRD patterns of the pellets with 5wt% C and 10wt% C electrolyzed for different durations.

In the second stage of the process after the first 2h of reduction, it is characterized typically by the decrease of CaTiO_3 peaks and the increase of the $\text{Ti}_x\text{O}_{1-x}$ peaks. The phase $\text{Ti}_x\text{O}_{1-x}$ was reported during the carbothermic reduction of TiO_2 ^[22, 23], but the operating temperature in the current work should be too low to form such the compound. Based on the results of the first stage of electrochemical reduction of

cathode, the formation of the oxycarbide phase can be described by equation (11). Fig.5 shows the variation of the lattice parameter of $\text{TiC}_x\text{O}_{1-x}$ with time of electrochemical reduction. The growth of lattice parameter values suggests that the oxygen/carbon ratio decreases with the increasing of reducing time. It can be deduced that oxygen atoms in $\text{TiC}_x\text{O}_{1-x}$ are substituted gradually by carbon atoms during the second stage, until the stoichiometric TiC is formed finally. By comparing the lattice parameter value of $\text{TiC}_x\text{O}_{1-x}$ in the same reducing time for the two samples with the different carbon contents, it shows that the higher content of carbon in the cathode, the faster rate of the transfer from TiO to TiC. The reaction described in equation (11) is the synergetic process of electrochemical reduction and carbiding. It indicates that the solid diffusion of carbon in the cathode should be the rate-determining step for carbide formation from the titanium monoxide.

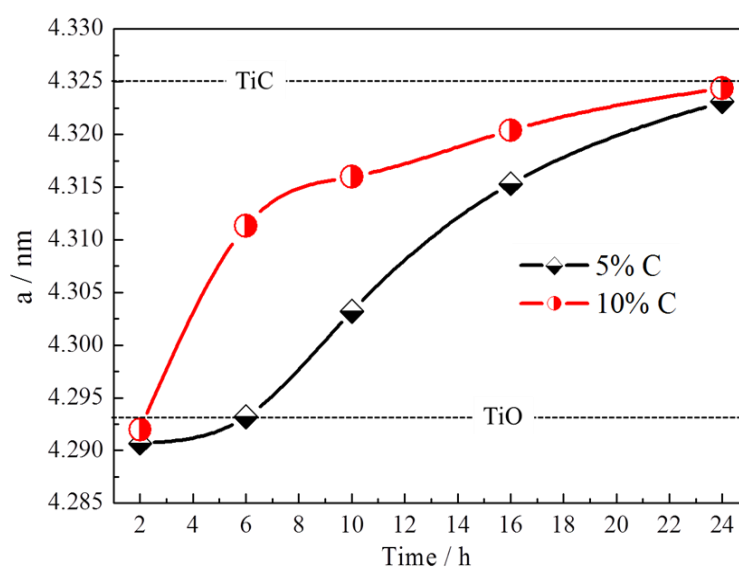
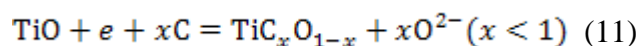
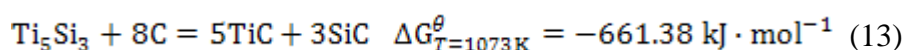
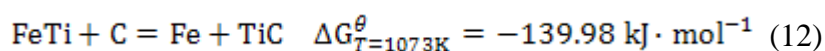


Fig.5 Changes of the lattice parameter of the phase $\text{TiC}_x\text{O}_{1-x}$ with time of electrochemical reduction.

In the middle of the second stage, the typical peaks of the alloys of FeTi and Ti_5Si_3 can be detected in Fig.4 for the carbon content of 5wt% and 10wt%, respectively. However, the alloys of FeTi and Ti_5Si_3 are the final metallic phases for the sample with 5wt% C, while the typical peaks of these alloys are eliminated for the sample with 10wt% C. It illustrates that the alloys are the intermediates which can be substituted by their carbides finally, and Fe is left in the metallic phase. The substitution reactions can be described as equation (12) and (13).



The transfer of the alloys to their carbides for the sample with the more carbon also indicates the reduction of the oxides within the cathode is much faster than carbiding in the second stage.

3.4 Microstructures of reduced samples

Fig. 6(a) shows the morphology of the pellet containing 5wt% carbon electrolyzed at 800°C for 24 h. These particles are around 2 μm in size with a smooth surface, and are even lightly sintered and connected one other. Fig.6(b) is the back-scattered micrograph of the cross-section of particle shown in Fig.6(a). In combination of the EDS results shown in Fig.6(c) and (d), it is reasonable to conclude that TiC particles are mostly located inside the large alloy nodules. To measure the particle size of TiC, the product was leached with 36% HCl aqueous solution at 70°C for 2h to dissolve metal matrix. Fig. 6(e) and (f) are the SEM image of the sample after the leaching process, and the EDS result of the labeled area in Fig. 6(e), respectively. The results

indicate that the particle size of TiC is less than 100nm. It can be deduced that the relatively low temperature and the surrounding Fe-based alloy decrease the driving force for TiC grain growth and prevent the occurrence of sintering among the TiC particles to form large ones. Although the temperature of the melt is 800°C, which is much lower than the melting point of TiFe or Ti₅Si₃, the carbiding reaction in the process is an exothermic reaction, and the heat released can make the local temperature rise in the micro-region around the TiC particles, and supply the impetus for FeTi grains to grow larger with TiC particles which serve as the nuclei for heterogeneous nucleation. Considering the composition of the slag and 5wt% C in the starting material, if neglecting the carbon loss during the sintering process, the final product of TiC-Fe based alloy powder is composed of around 40wt% carbide phase (TiC) and 60 wt% metallic phase (TiFe and Ti₅Si₃).

Fig. 7(a) and (b) show the SEM image of the pellet containing 10 wt% carbon electrolyzed at 800°C for 24 h, and the EDS result of the labeled area in Fig.7(a), respectively. The composite powder has the particles of around 300nm in size. According to the typical XRD pattern shown in Fig. 4(b), it mainly composed of TiC/SiC and Fe, and the content of Fe in the product is less than around 9 wt%, and the rest is 91 wt% carbides (TiC and SiC). Therefore, this less amount of iron can only supply the thin shell over the carbide particles. Fig. 7(c) and (d) show the SEM image of the composite powder after the post-leaching process, and the EDS result of the labeled area in Fig. 7(c), respectively. Comparing the particles shown in Fig.6 (e), the TiC grains from the precursor containing 10% carbon are aggregated together to

form larger ones, The aggregation of TiC grains should be due to the fact that the amount of metal phase is too few to disperse the TiC grains. Therefore, the amount of metal phase in the TiC-Fe based composite powder can be adjusted to prevent TiC grains from aggregating. Fine TiC particles as a reinforcing phase can increase the wear resistance of the composite material.

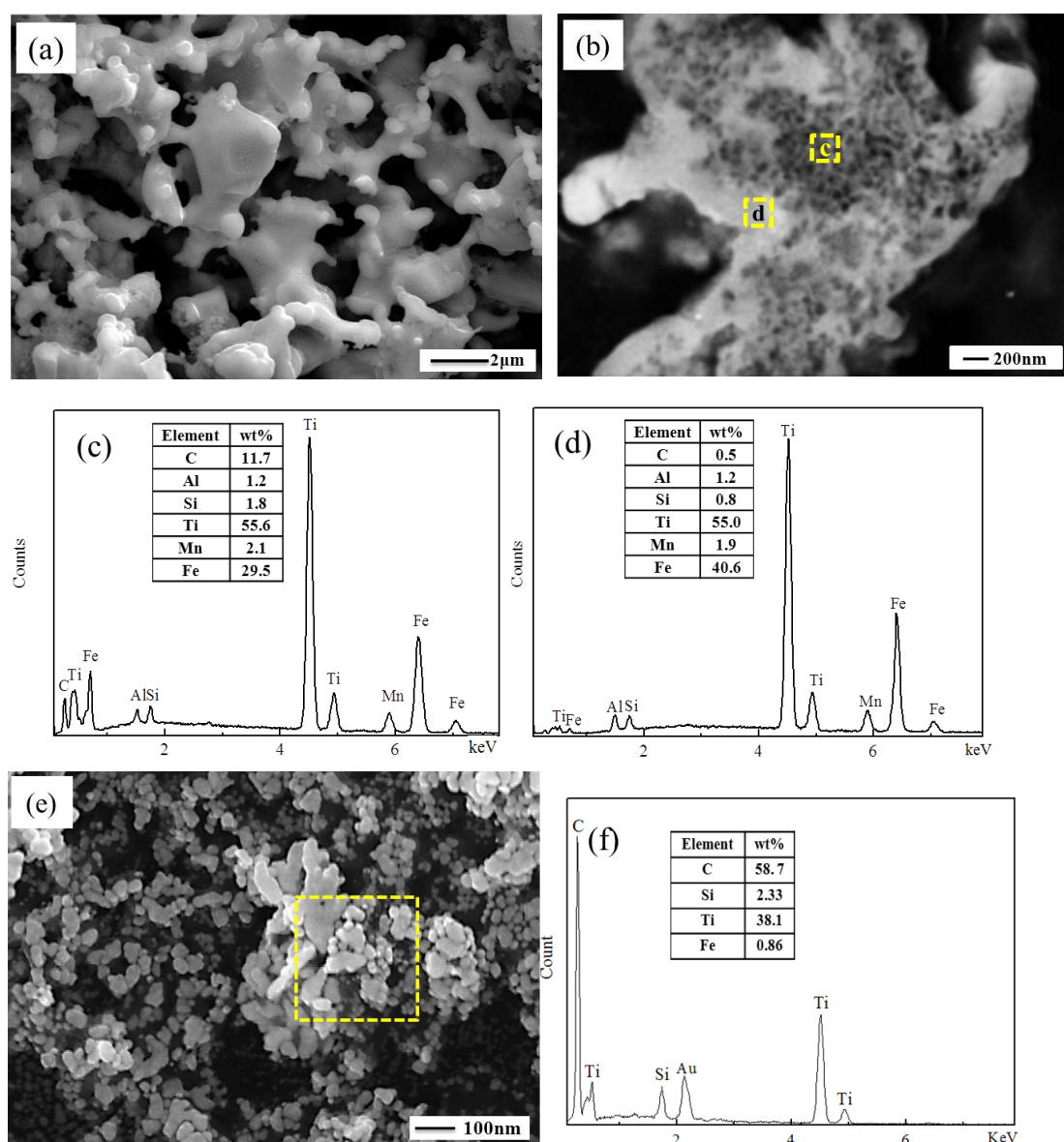


Fig.6. (a)SEM image of the pellet with 5wt% C electrolyzed for 24h; (b)SEM back-scattering image of the cross-section of particle in Fig.6 (a); (c) EDS result of the labeled area 'c' in Fig.6 (b); (d) EDS result of the labeled area 'd' in Fig.6 (b). (e) SEM image of the sample obtained from the pellet with 5wt% C electrolyzed for 24h after leaching process. (f) EDS result of the labeled area in Fig.6 (e)

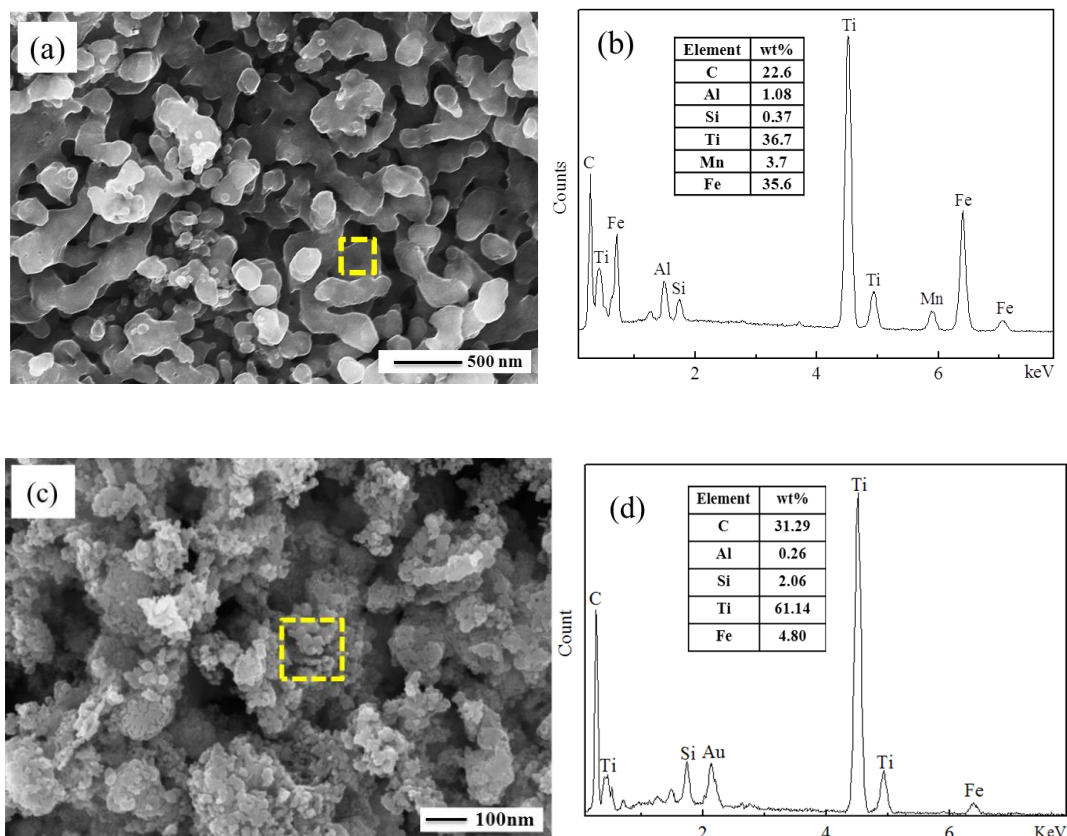


Fig.7(a) SEM image of the pellet with 10wt% C electrolyzed for 24h;(b) EDS result of the labeled area in Fig.7 (a). (c) SEM image of the powder obtained from the pellet with 10wt% C electrolyzed for 24h after leaching process. (d) EDS result of the labeled area in Fig.6 (c)

4. Conclusions

TiC reinforced Fe based composite powder is electrochemically prepared directly from the titanium-rich slag and carbon in molten $\text{CaCl}_2\text{-NaCl}$ at $800\text{ }^\circ\text{C}$. The composition of the carbides can be controlled by adjusting of the amount of carbon in the titanium-rich slag. The reaction pathway obtained by interrupting the reduction process after different times, can be divided into the two stages. The first stage is the electrochemical reduction of the titanium-rich slag and formation of elementary Fe, TiO and CaTiO_3 , and the second stage is the synergetic process of electrochemical reduction and carbiding. During the second stage, TiC forms from $\text{TiC}_x\text{O}_{1-x}$, which

successively increases its carbon content till the formation of stoichiometric TiC finally. The TiC grains can serve as the nuclei of heterogeneous nucleation for the TiC-Fe based composite particles with multi-core microstructure.

Acknowledgements

The authors acknowledge the National Natural Science Foundation of China (Grant No.50874026 and 51404057), the China Postdoctoral Science Foundation (Grant No.2013M530935) and the fundamental Research Funds for the Central Universities (N120302007), China for financial supports.

References

- [1] E. Pagounis, M. Talvitie, V. K. Lindroos, *Metall. Mater. Trans. A.*, 1996, 27A, 4171-4181.
- [2] H. Seilstorfer, G. Moser, *Metall.*, 1980, 10, 925-929.
- [3] E. Pagounis, M. Talvitie, V. K. Lindroos, *Powder. Metall.*, 1997, 40, 55-61.
- [4] K. Das, T. K. Bandyopadhyay, S. Das, *J. Mater. Sci.*, 2002, 37, 3881-3892.
- [5] T. Z. Kattamis, T. Suganuma, *Mater. Sci. Eng. A.*, 1990, 128, 241-252.
- [6] B. S. Terry, O. S. Chinyamakobvu, *J. Mater. Sci. Lett.*, 1991, 10, 628-629.
- [7] N. J. Welham, *Miner. Eng.* 1996. 9 (12), 1189-2000.
- [8] A. Saidi, A. Chrysanthou, J. V. Wood, J. L. F. Kellie, *J. Mater. Sci.*, 1994, 29, 4993-4998.
- [9] P. A. Persson, E. W. Jarfors, S. Savage, *J. Mater. Proc. Technol.*, 2002. 127, 131-139.
- [10] W. F. Zhang, X. H. Zhang, J. L. Wang, C. Q. Hong, *Mater. Sci. Eng. A.*, 2004,

381, 92-97.

[11] D. D. Gu, Z. Y. Wang, Y. F. Shen, Q. Li, Y. F. Li, *Appl. Surf. Sci.*, 2009, 255, 9230-9240.

[12] M. Razavi, M. R. Rahimpour, A. H. Rajabi-Zamani, *J. Alloy. Compd.*, 2007, 436, 142-145.

[13] G.Q. Zhang, D. D. Gu, *Appl. Surf. Sci.*, 2013, 273, 364-371.

[14] S.Y. Ahn, S. Kang, *J. Am. Ceram. Soc.*, 2000, 83, 1489-1494.

[15] S. Kim, K. Min, S. Kang, *J. Am. Ceram. Soc.* 2003, 86, 1761-1766.

[16] H. Kwon, S. Kang, *Mater. Sci. Eng. A.*, 2009, 520, 75-79.

[17] G. Z. Chen, D. J. Fray, T.W. Farthing, *Nature.*, 2000, 407, 361-364.

[18] X.Y. Yan, D. J. Fray, *J. Electrochem. Soc.* 2005, 152, 308-318.

[19] G. Z. Chen, E. Gordo, D. J. Fray, *Metall. Mater. Trans. A.*, 2004, B35, 223-233.

[20] A. M. Abdelkader, D. J. Fray, *J. Eur. Ceram. Soc.*, 2012, 32, 4481-4487.

[21] Q. S. Song, Q. Xu, R. Tao, X. Kang. *Int. J. Electrochem. Sci.*, 2012, 7, 272- 281.

[22] L.M. Berger, W. Gruner, E. Landgholf, S. Stolle, *Int. J. Refract. Met. Hard Mater.*, 1999, 17: 235-243.

[23] A. Afir, M. Achour, N. Saoula, *J. Alloys Compd.*, 1999, 288: 124-140.